

Optimization of multiple filamentation of femtosecond laser pulses in air using a pinhole

Zuo-Qiang Hao¹, Jie Zhang^{1,2*}, Ting-Ting Xi¹, Xiao-Hui Yuan^{1,3}, Zhi-Yuan Zheng¹, Xin Lu¹, Ming-Young Yu⁴, Yu-Tong Li¹, Zhao-Hua Wang¹, Wei Zhao³, Zhi-Yi Wei¹

¹Beijing National Laboratory for Condensed Matter Physics, Institute of Physics, Chinese Academy of Sciences, Beijing 100080, China

²Department of Physics, Shanghai Jiao Tong University, Shanghai 200240, China

³State Key Laboratory of Transient Optics Technology, Xi'an Institute of Optics and Precision Mechanics, Chinese Academy of Sciences, Xi'an 710068, China

⁴Theoretical Physics I, Ruhr-University Bochum, D-44780 Bochum, Germany

*Corresponding author: jzhang@aphy.iphys.ac.cn

Abstract: The robustness and prolongation of multiple filamentation (MF) for femtosecond laser propagation in air are investigated experimentally and numerically. It is shown that the number, pattern, propagation distance, and spatial stability of MF can be controlled by a variable-aperture on-axis pinhole. The random MF pattern can be optimized to a deterministic pattern. In our numerical simulations, we configured double filaments to principally simulate the experimental MF interactions. It is experimentally and numerically demonstrated that the pinhole can reduce the modulational instability of MF and is favorable for a more stable MF evolution.

©2007 Optical Society of America

OCIS codes: (190.5530) Pulse propagation and solitons; (320.7110) Ultrafast nonlinear optics.

References and links

1. A. Braun, G. Korn, X. Liu, D. Du, J. Squier, and G. Mourou, "Self-channeling of high-peak-power femtosecond laser pulses in air," *Opt. Lett.* **20**, 73-75 (1995).
2. L. Wöste, C. Wedekind, H. Wille, P. Rairoux, B. Stein, S. Nikolov, C. Werner, S. Niedermeier, F. Ronneberger, H. Schillinger, and R. Sauerbrey, "Femtosecond atmospheric lamp," *Las. Optoelektron.* **29**, 51-53 (1997).
3. S. L. Chin, F. Théberge, and W. Liu, "Filamentation nonlinear optics," *Appl. Phys. B* **86**, 477-483 (2007).
4. H. Schillinger and R. Sauerbrey, "Electrical conductivity of long plasma channels in air generated by self-guided femtosecond laser pulses," *Appl. Phys. B* **68**, 753-756 (1999).
5. S. Tzortzakis, M. A. Franco, Y. -B. André, A. Chiron, B. Lamouroux, B. S. Prade, and A. Mysyrowicz, "Formation of a conducting channel in air by self-guided femtosecond laser pulses," *Phys. Rev. E* **60**, R3505-3507 (1999).
6. G. Méchain, A. Couairon, M. Franco, B. Prade, and A. Mysyrowicz, "Organizing multiple femtosecond filaments in air," *Phys. Rev. Lett.* **93**, 035003 (2004).
7. J. Kasparian, R. Sauerbrey, D. Mondelain, S. Niedermeier, J. Yu, J. -P. Wolf, Y. -B. André, M. Franco, B. Prade, S. Tzortzakis, A. Mysyrowicz, M. Rodriguez, H. Wille, and L. Wöste, "Infrared extension of the supercontinuum generated by femtosecond terawatt laser pulses propagating in the atmosphere," *Opt. Lett.* **25**, 1397-1399 (2000).
8. Z. Q. Hao, J. Zhang, Z. Zhang, X. H. Yuan, Z. Y. Zheng, X. Lu, Z. Jin, Z. H. Wang, J. Y. Zhong, and Y. Q. Liu, "Characteristics of multiple filaments generated by femtosecond laser pulses in air: Prefocused versus free propagation," *Phys. Rev. E* **74**, 066402 (2006).
9. J. Kasparian, M. Rodriguez, G. Méjean, J. Yu, E. Salmon, H. Wille, R. Bourayou, S. Frey, Y. -B. André, A. Mysyrowicz, R. Sauerbrey, J. -P. Wolf, and L. Wöste, "White-light filaments for atmospheric analysis," *Science* **301**, 61-64 (2003).
10. S. Eisenmann, E. Louzon, Y. Katzir, T. Palchan, A. Zigler, Y. Sivan, and G. Fibich, "Control of the filamentation distance and pattern in long-range atmospheric propagation," *Opt. Express* **15**, 2779-2784 (2007), <http://www.opticsexpress.org/abstract.cfm?URI=OPEX-15-6-2779>.
11. E. Esarey, P. Sprangle, J. Krall, and A. Ting, "Self-focusing and guiding of short laser pulses in ionizing gases and plasmas," *IEEE J. Quantum Electron.* **33**, 1879-1914 (1997).
12. B. La Fontaine, F. Vidal, Z. Jiang, C. Y. Chien, D. Comtois, A. Desparois, T. W. Johnston, J. -C. Kieffer, H. Pépin, and H. P. Mercure, "Filamentation of ultrashort pulse laser beams resulting from their propagation over long distances in air," *Phys. Plasmas* **6**, 1615-1621 (1999).

13. H. Yang, J. Zhang, Y. J. Li, J. Zhang, Y. T. Li, Z. L. Chen, H. Teng, Z. Y. Wei, and Z. M. Sheng, "Characteristics of self-guided laser plasma channels generated by femtosecond laser pulses in air," *Phys. Rev. E* **66**, 016406 (2002).
14. M. Mlejnek, M. Kolesik, J. V. Moloney, and E. M. Wright, "Optically turbulent femtosecond light guide in air," *Phys. Rev. Lett.* **83**, 2938-2941 (1999).
15. L. Bergé, S. Skupin, F. Lederer, G. Méjean, J. Yu, J. Kasparian, E. Salmon, J. P. Wolf, M. Rodriguez, L. Wöste, R. Bourayou, and R. Sauerbrey, "Multiple filamentation of terawatt laser pulses in air," *Phys. Rev. Lett.* **92**, 225002 (2004).
16. S. Tzortzakis, L. Bergé, A. Couairon, M. Franco, B. Prade, and A. Mysyrowicz, "Breakup and fusion of self-guided femtosecond light pulses in air," *Phys. Rev. Lett.* **86**, 5470-5473 (2001).
17. A. Dubietis, G. Tamošauskas, G. Fibich, and B. Ilan, "Multiple filamentation induced by input-beam ellipticity," *Opt. Lett.* **29**, 1126-1128 (2004).
18. G. Fibich and B. Ilan, "Deterministic vectorial effects lead to multiple filamentation," *Opt. Lett.* **26**, 840-842 (2004).
19. G. Fibich, S. Eisenmann, B. Ilan, and A. Zigler, "Control of multiple filamentation in air," *Opt. Lett.* **29**, 1772-1774 (2004).
20. A. Talebpour, S. Petit, and S. L. Chin, "Re-focusing during the propagation of a focused femtosecond Ti:Sapphire laser pulse in air," *Opt. Commun.* **171**, 285-290 (1999).
21. Z. Q. Hao, J. Zhang, J. Yu, Z. Zhang, J. Y. Zhong, C. Z. Zang, Z. Jin, Z. H. Wang, and Z. Y. Wei, "Fluorescence measurement and acoustic diagnostics of plasma channels in air," *Acta Phys. Sin.* **55**, 299-303 (2006).
22. W. Liu, F. Théberge, E. Arévalo, J. -F. Gravel, A. Becker, and S. L. Chin, "Experiment and simulations on the energy reservoir effect in femtosecond light filaments," *Opt. Lett.* **30**, 2602-2604 (2005).
23. Z. Q. Hao, J. Zhang, X. Lu, T. T. Xi, Y. T. Li, X. H. Yuan, Z. Y. Zheng, Z. H. Wang, W. J. Ling, and Z. Y. Wei, "Spatial evolution of multiple filaments in air induced by femtosecond laser pulses," *Opt. Express*, **14**, 773-778 (2006), <http://www.opticsexpress.org/abstract.cfm?URI=OPEX-14-2-773>.
24. T. T. Xi, X. Lu, and J. Zhang, "Interaction of light filaments generated by femtosecond laser pulses in air," *Phys. Rev. Lett.* **96**, 025003 (2006).
25. S. A. Hosseini, Q. Luo, B. Ferland, W. Liu, S. L. Chin, O. G. Kosareva, N. A. Panov, N. Aközbek, and V. P. Kandidov, "Competition of multiple filaments during the propagation of intense femtosecond laser pulses," *Phys. Rev. A* **70**, 033802 (2004).
26. Q. Luo, S. A. Hosseini, W. Liu, J. -F. Gravel, O. G. Kosareva, N. A. Panov, N. Aközbek, V. P. Kandidov, G. Roy, and S. L. Chin, "Effect of beam diameter on the propagation of intense femtosecond laser pulses," *Appl. Phys. B* **80**, 35-38 (2004).
27. V. P. Kandidov, O. G. Kosareva, M. P. Tamatov, A. Brodeur, and S. L. Chin, "Nucleation and random movement of filaments in the propagation of high-power laser radiation in a turbulent atmosphere," *Quantum Electron.* **29**, 911-915 (1999).

1. Introduction

The propagation of ultra-intense femtosecond (fs) laser pulses in air has been extensively investigated recently in view of many potential applications such as lightning control and remote sensing of the atmosphere [1-10]. For a laser beam at a wavelength $\lambda = 800$ nm, when the laser power exceeds the critical value $P_{crit} = \lambda^2 / 2\pi n_0 n_2$ of about 3.2 GW [11], nonlinear Kerr self-focusing of the laser beam occurs and the increased intensity at the focus can cause multiphoton ionization (MPI) of molecules in air. The resulting electron generation contributes negatively to the index of refraction of air, namely $n_{plasma} = -\omega_p^2(r) / 2\omega^2$, where $\omega_p = (4\pi e^2 n_e / m_e)^{1/2}$ is the plasma frequency and n_e is the electron density. This will defocus the laser beam [11]. A dynamic balance between these two effects could then follow, leading to very-long filament propagation, exceeding many Rayleigh lengths of the laser beam. Usually, the light intensity inside the filaments is about $5 \times 10^{13} - 1 \times 10^{14}$ W/cm² [12] and the electron density is about $10^{16} - 10^{18}$ cm⁻³ [9, 13], so that the filaments are conductive [4, 5]. Often, one finds that there is more than one filament in the beam, indicating laser- or plasma-induced inhomogeneity of the beam. The dynamics of the filamentation process is in fact rather complicated and the physics of multiple filamentation (MF) formation and evolution is still not well understood. Apart from the Kerr self-focusing and plasma defocusing, other

nonlinear effects, such as self-phase modulation, four-wave mixing, stimulated Raman scattering, etc. can also play important roles.

Mlejnek et al. proposed a model of optical turbulent light guiding to explain the breakup and fusion of filaments [14]. This was confirmed experimentally by Bergé et al [15]. Tzortzakis et al. proposed that the main mechanism is the modulational instability (MI) of laser pulses [16]. Besides, the stability of MF is also affected by the ellipticity [17] and vectorial effects [18] of the initial laser beam. The apparently random MF can be harmful in applications where precise localization of the beam is required. Méchain et al. realized the organized MF using a trefoil or a fivefoil diaphragm [6]. Fibich et al. obtained a single filament with highly pointing stability by using a tilted lens setup [19]. In this paper, we propose an alternative approach to form more stable and longer filaments. We demonstrated that when the cross section of the plasma channel is restricted by a pinhole, remarkably robust and prolonged filaments are attained. The intensity and propagation distance of the filament are controllable by varying the aperture of the pinhole. Our simulations retrieve the phenomenon that the filaments can be prolonged and stabilized, which is in good agreement with experimental results.

2. Experimental setup and results

The laser used is a Ti:sapphire laser system, Xtreme Light II (XL-II), with an output energy of up to 640 mJ in 30 fs duration. The central wavelength is 800 nm and the repetition rate is 10 Hz. In the experiments, a laser pulse of energy 15 mJ is focused by an $f = 200$ cm convex lens. The experimental setup is shown in Fig. 1. The laser beam is focused in air and forms a long plasma channel that can be observed directly by naked eyes. A charged-coupled device (CCD) camera (512×512 pixels) with a pixel size of 24 μm records the beam cross-section at 520 cm and 690 cm distance from the lens. Another CCD camera records the beam along the laser axis. Filters with a wavelength range of $350 \text{ nm} < \lambda < 500 \text{ nm}$ are used at both CCD cameras to reduce the scattering noise from the pump laser. A typical profile of the plasma channel is shown in Fig. 2. Because of the Kerr self-focusing, the laser beam focuses before the geometrical focus which is indicated by the arrow in the figure. A pinhole as long as 4 mm in a copper plate (see the inset of Fig. 1) is centered on the beam axis at $Z_0 = 190$ cm. The purpose of using the relative long pinhole is to effectively eliminate the small filaments with large angle to the main ones. The axial and transverse profiles of the plasma filaments are measured directly by the two CCD cameras.

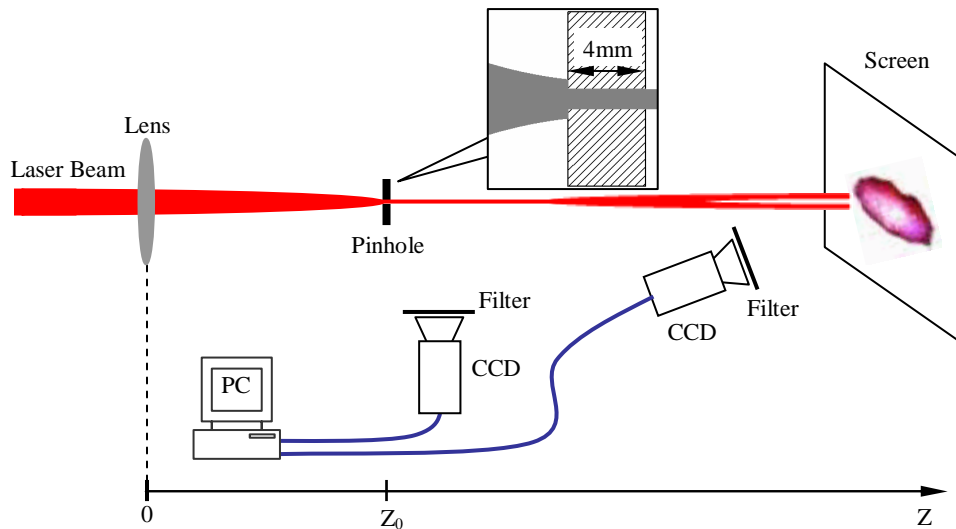


Fig. 1 Schematic diagram of the experimental setup. $Z_0 = 190$ cm is the position of the pinhole. The insert shows the copper pinhole.

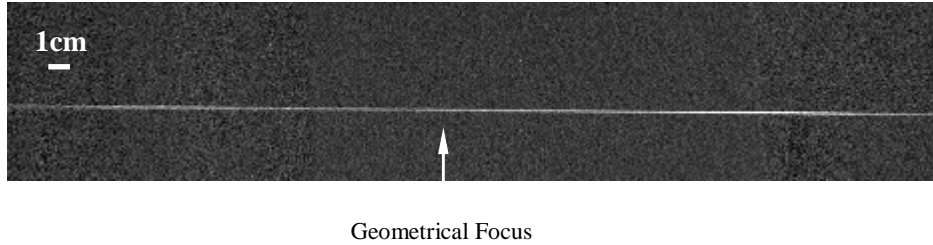


Fig. 2 A typical profile of the plasma channel with laser energy of 35 mJ. The position of the arrow is the geometrical focus.

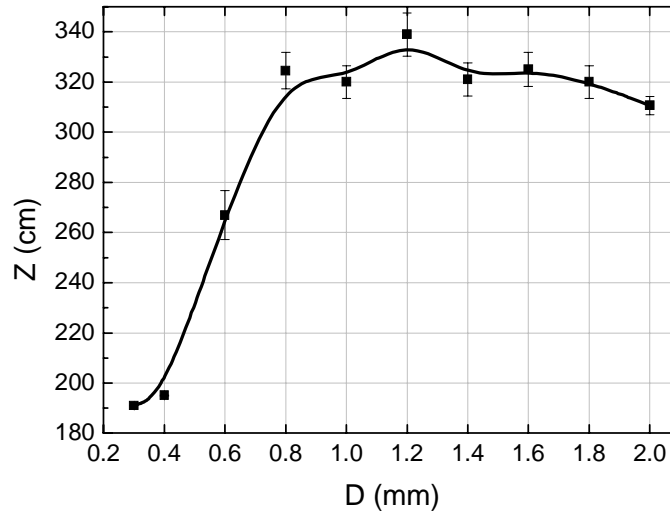


Fig. 3 The filaments propagation distance from the lens versus the diameter of the pinhole.

In the experiments, 15 mJ of laser pulse energy, corresponding to a peak power of about 500 GW, is used. This power is significantly higher than the critical power for self-focusing. A long plasma channel begins to form at about 170 cm after the convex lens. The fluorescence emitted from excited nitrogen molecules in the channel can be observed directly by naked eyes [20, 21]. Therefore, the filamentation process can be visualized by the observation of the fluorescence, and we can image it by the CCD cameras. To control the diameter of the channel, a pinhole with variable apertures is placed at the center of the laser beam axis. In our experiments condition, the pinhole position $Z_0 = 190$ cm is the optimized choice to study the filaments. We find that if the distance between the lens and the pinhole is smaller, there is no chance for filaments to develop into mature ones. The filaments will decay fast due to the lack of laser energy. However, if the distance is too large, some dynamic interactions have already harmfully influenced the MF. As a result, the MF cannot be effectively controlled by the pinhole setup. Therefore, we chose $Z_0 = 190$ cm of the pinhole position, which results in a remarkable phenomenon that the intensity of the fluorescence from the filaments becomes brighter and the propagation distance of the filaments longer when a pinhole between 0.8 and 1.8 mm in diameter is inserted. Figure 3 shows the dependence of the propagation distance Z of the MF on the diameter D of the pinhole. When the diameter of the pinhole is $D = 0.3$ and 0.4 mm, the filament is almost terminated and its length is only several centimeters beyond the pinhole, as Liu et al. observed [22]. The longest filament occurs for $D = 1.2$ mm, corresponding to a channel distance of beyond 340 cm. When $D \geq 2.0$ mm, the pinhole has no observable effect on the filaments since almost the entire laser beam can get through. In the absence of the pinhole, the measured propagation distance of filaments is about 310 cm. That

is, the plasma channel can be prolonged by inserting a pinhole of appropriate aperture along the optical axis.

The important role of the pinhole lies in not only the prolongation of MF, but also the stability of the MF. The traverse profiles of the MF at $Z = 520$ and 690 cm are recorded by the second CCD camera. Figure 4 shows the spatial variation of the filaments as a function of the aperture of the pinhole.

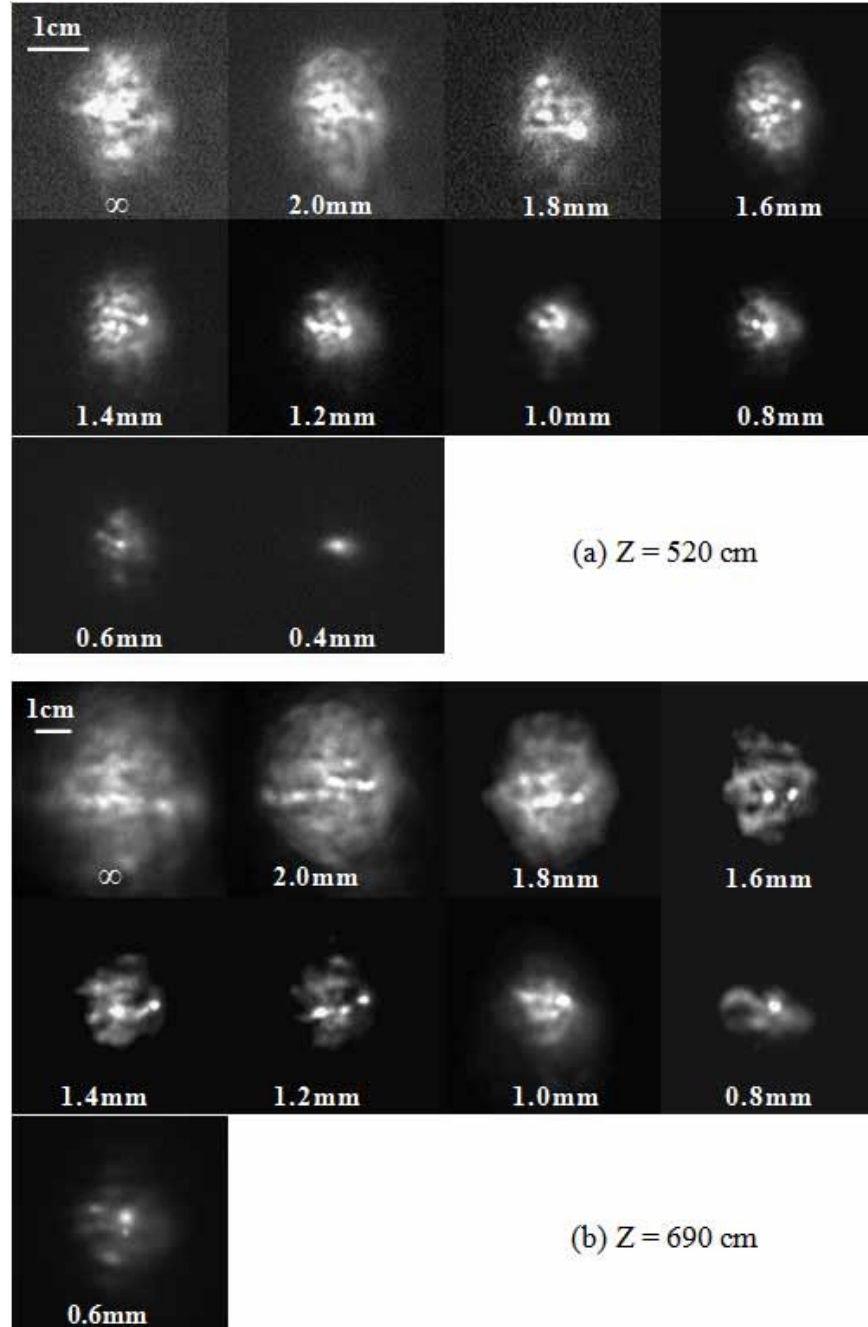


Fig. 4 Typical traverse filamentation patterns at $Z = 520$ cm (a) and $Z = 690$ cm (b) versus the diameter of the pinhole.

Figure 4(a) shows the MF patterns for different diameters of the pinhole. The first image is for a free propagation without any pinhole. We see that the beam is dispersed into a relatively large area showing several bright spots. The positions of these spots are unfixed from shot to shot. As we limit the plasma channel by pinholes of diameters from 2.0 to 0.8 mm, the laser beam cross section becomes smaller, and the number, position, and intensity of the filaments change. When the diameter is 1.6 mm, the filaments are robust and distinct from each other. With further decrease of the diameter, the number of filaments becomes less. When the pinhole diameter is 0.8 mm, there are only two filaments, one large and one small. All the pinhole controlled MF patterns are reproducible. Finally, for $D < 0.6$ mm we observe only a dispersed light spot. We can conclude that the MF patterns for $D = 1.6 - 0.8$ mm are highly stable and reproducible. The number and locations of the MF rarely change from shot to shot.

At $Z = 690$ cm, as shown in Fig. 4(b), the dependence of the MF profiles on the pinhole aperture is similar to the case of 520 cm distance. Comparing the MF patterns at two distances, we see that the differences are only in the number, intensity, and spatial extent of the filaments. From the MF patterns at the two positions, we can also infer the longitudinal evolution of the MF. For example, at 690 cm there are only two intense filaments for $D = 1.6, 1.4$ and 1.2 mm, and a single stable filament for $D = 0.8$ mm. These numbers are less than that observed at 520 cm, indicating that some filaments have terminated or combined.

It is noted that the free propagation MF generated in our experiments is not stable compared with our recent experiments used a longer focal length ($f = 400$ cm) lens [23]. Our theoretical investigation verified that the difference should be dependent on the focus of the lens. The stability of the MF has a close relationship on the incident angle of two plasma filaments [24]. Therefore, the MF generated by a lens with shorter focal length will boost stronger instability.

3. Numerical simulation and discussion

The propagation of an fs laser pulse in air can be described by an extended nonlinear Schrödinger equation (NLS) coupled with electron density of plasma due to MPI, which governs the slowly varying envelope of the linearly polarized laser electric field in the frame moving with the laser pulse. We solved the coupled equations by use of faster Fourier transformation in time and Crank-Nicholson arithmetic in space. The detail description of the model can be found elsewhere [24]. In Ref [24], we generated a light bullet at 200 cm, based on which we studied the various interactions of two filaments. In this paper, we perform the numerical simulations also based on the light bullet formed in Ref [24]. In order to show the scene of MF interactions observed in our experiments, we configure two filaments with a separation of 0.5 mm, incident angle of 0.2° and the same phase. However, they have different initial intensities. Starting from the light bullet used in Ref [24], we numerically generate another one with a half intensity of the original. The stronger one simulates the main filament, and the weaker one simulates the small-scale filament surround the main filament. Further, we insert a diaphragm with different diameters. The energy fluence of the light filaments with different diameter of diaphragm is shown in Fig. 5. The evolution of the MF is strongly affected by the pinholes. When no pinhole is used, the MF decays quickly with less stability. It continues propagation no less than 35 cm. However, the MF becomes longer and more robust when a pinhole is inserted to restrict the filament diameter. When the diameter of pinhole increases from 0.4 mm to 1.0 mm, larger of the diameter is, longer and more robust of the MF is. When we continue to enlarge the pinhole diameter to 1.2 – 1.8 mm, the propagation of the MF exhibits obvious instabilities as the free propagation does. However, in this case the MF can propagation at longer distance with less continuity in the propagation direction. The $D = 2$ mm pinhole does not remarkably affect the MF propagation, compared to the free propagation case. Furthermore, when we put the pinhole at the 5 cm and 10 cm from the initial position respectively, as shown in Fig. 5(k) and (l), there is no obvious effect to the evolution of the double filaments, which is coincide with our experiments observation.

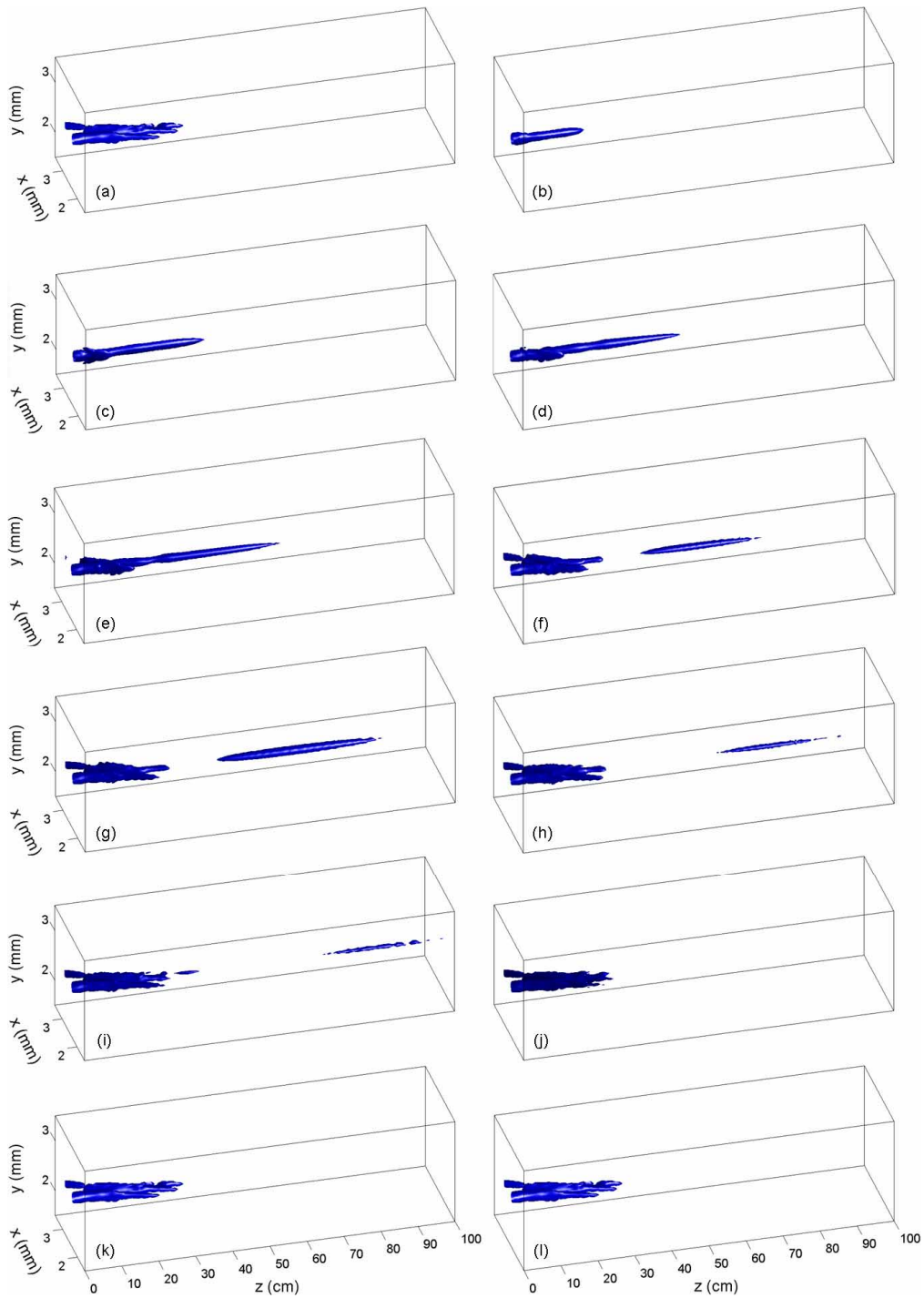


Fig. 5 The energy fluence distribution ($\text{fluence}_{\text{iso}}=1.65$) of the configured double filaments along the propagation direction when the insert diaphragm diameter is ∞ (without pinhole) (a); 0.4 mm (b); 0.6 mm (c); 0.8 mm (d); 1.0 mm (e); 1.2 mm (f); 1.4 mm (g); 1.6 mm (h); 1.8 mm (i); 2.0 mm (j) at the initial distance (corresponding to $z_0 = 190$ cm in the experiment); 0.6 mm at the distance of 5 cm (k) and 10 cm (l) from the initial distance.

Therefore, in our simulations the 1.0 mm pinhole is the best one to stretch and strengthen the MF with high stability, which is very useful for laser-guided discharging and other related research fields. However, if we would rather obtain a longer MF with a relatively high intensity and less continuity, 1.4 mm pinhole should be the best choice.

Our previous theoretical investigation has demonstrated that the incident angle of two plasma filaments also plays an important role in MF interaction and propagation length [24]. With a small incident angle, 0.01° for example, two filaments fuse and form a stable one, while for a larger incident angle, 0.1° for example, the two filaments propagate along their own track after crossing, instead of merging into one. Hosseini et al. also investigated the competition of MF [25]. They found that the development of the plasma channel strongly depends on the intensity fluctuations in the beam profile and on the relative distance between the filaments. Closer the filaments are, more stable, stronger, and longer the filaments become [26]. However, because of the strong turbulence driven by the space-time collapse of the laser light, the filaments have a complicated structure. Some small filaments form because of the random nucleation effect during the propagation of filaments [27]. In order to eliminate the influence of the disordered filaments in the periphery of the plasma channel, we restrict the plasma channel using a pinhole. The MI is effectively reduced to a level that cannot affect the evolution of the main filaments, which can be seen from the Fig. 4 and 5. The pinhole seems to act as a spatial filter to clean up the laser by removing aberrations in the beam. Inside the pinhole, the remains of the small filament becomes too weak to harm the evolution of the main filament. At the same time, a part of energy of the small filament is attracted to the main filament. As a result, the main filament becomes longer and more robust than that in free propagation condition. Noted that the large length of the pinhole plays an important role in eliminating the filaments with large angle to the main filaments.

We note that in our simulations the double filaments evolved into a single filament after we added the pinhole with a diameter of 0.4 – 1.8 mm, as shown in Fig. 5. We achieved the cleaner MF patterns using the pinhole setup not only in experiment but also in simulation. We can conclude that the appropriate elimination of the disordered small filaments surrounding the main filaments results in the formation of cleaner, more stable and more robust MF patterns.

The pinhole aperture plays an important role in controlling the filaments. On the one hand, it reduces the turbulence in the periphery of the plasma channel and leads to relatively stable MF. On the other hand, it should allow enough energy through to feed the remaining filaments. In our experiments, the optimum diameter of the pinhole is 1.2 mm, and a deterministic MF pattern is obtained. In our simulations, the optimal pinhole diameter is 1.0 mm. The differences between them are mainly due to the different initial laser parameters and some simplifications in our numerical simulations.

4. Conclusions

In conclusion, the effect of an on-axis pinhole on the MF of an fs laser beam has been studied. For appropriate pinhole diameters, the MF can be stable, and propagates for a longer distance. By eliminating the disordered energy reservoir in the periphery of the plasma channel, the pinhole setup leads to a longer and more regular MF pattern. We configured double filaments in theory to simulate the phenomenon in our experiments. The numerical simulations retrieve the essential features of the experimental results. Further experimental and numerical optimization of filamentation enables one to achieve optimized or otherwise desired MF patterns, which are important for many research and practical applications.

Acknowledgments

This work was supported by the National Nature Science Foundation of China under Grant Nos. 10634020, 10390161, 60621063, and 60478047, and National Basic Research Program of China (973 Program) (Grant No. 2007CB815101).